Effect of Aggressive Ions on Degradation of WE43 Magnesium Alloy in Physiological Environment

Xuehua Zhou[1, 2], Li Jiang[1,*], Panpan Wu[1], Yi Sun[1], Yundan Yu[1], Guoying Wei[1], Hongliang Ge[1]

[1] College of Materials Science and Engineering, China Jiliang University, Hangzhou, China
[2] Shanghai Institute of Microsystem And Information Technology, Chinese Academy of Sciences, Shanghai,China.
[*]E-mail: jiangliwhu@126.com

Influences of chloride, sulfate, dihydrogen phosphate and bicarbonate anion in simulated blood fluid (SBF) on the corrosion behavior of WE43 alloy were investigated using electrochemical techniques. In the initial stage, as the concentration of $[Cl^-]$, $[SO_4^{2-}]$, $[H_2PO_4^-]$ and $[HCO_3^-]$ increased, the open circuit potential (E_{ocp}) and corrosion potential (E_{corr}) of WE43 alloy specimens shifted to the negative direction, and corrosion current density (I_{corr}) increased, accounted for the greater activity of alloy. The order of ions corrosivity for WE43 alloy immersed in SBF was $Cl^- > SO_4^{2-} > HCO_3^- > H_2PO_4^-$. Through the analysis of electrochemical impedance spectroscopy (EIS), the corrosion mechanism and equivalent circuit models were discussed. Corrosion process of WE43 alloy in NaCl solution was different from others. Its surface exhibited the characteristics of electric double layer, surface oxide film and the occurrence of pitting corrosion respectively. Corrosion phenomenon was much pronounced in the solution containing Cl^- and SO_4^{2-} ions. Moreover, WE43 alloy had better corrosion resistance in NaH_2PO_4 solution, attributed to the lower concentration of $[H_2PO_4^-]$ in SBF.

1. INTRODUCTION

In the field of bioabsorbable implant materials, magnesium (Mg) has become an interesting candidate as a bioactive substance which naturally degrades with the body. Mg is an essential element in the human body, it degrades in aqueous solutions and its mechanical properties are more advantageous than those of degradable polymeric materials [1]. In recent studies, WE43 (nominally 4 wt% Y and 3 wt% RE) alloy has been found to meet many requirements for implant applications [2-4]. It features excellent mechanical properties and high corrosion resistance combined with light weight [5]. The animal and clinical experiment results show that the WE43 alloy stents possessed sufficient

anti-proliferative properties and drastically reduced the restenosis rate in comparison to conventional stainless steel stents [6].

In the material selection and design of degradable bone plates, the knowledge of implants' corrosion rate in body fluids is of paramount importance. It provides baseline information in materials development or surface modification for enhancing the corrosion resistance of degradable implants. For the application of Mg as medical implant material, simulated blood fluid (SBF) is used as test electrolyte. Many ions such as Cl^-, HCO_3^-, SO_4^{2-}, Ca^{2+}, etc. exist in SBF, and some of them have great importance on the corrosion performance of Mg alloys. In the literatures, many studies of Mg alloy focused on the role of Cl^- ion in the corrosion process. Cl^- ion has a pronounced effect on the corrosion rate of Mg [7, 8], in particular the anodic dissolution mechanism. Phosphates (HPO_4^{2-}, PO_4^{3-}) and carbonates (HCO_3^-, CO_3^{2-}) ions were also detected to be involved in the corrosion mechanism and incorporated in the corrosion layer on bioactive materials [9], However, their effects on corrosion of Mg alloys are unknown. In the paper, influence of Cl^-, SO_4^{2-}, HCO_3^- and $H_2PO_4^-$ ions in physiological environment on the corrosion behavior and mechanism of WE43 alloy were detailed studied.

2. MATERIALS AND METHODS

Experiments were performed on an extruded WE43 Mg alloy. Materials specifications are given in Table 1, according to ASTM designations. The test specimens were columnar in shape with the dimension of 12mm×12mm×10mm. The specimens were connected to Cu wires and embedded in epoxy resins except the exposed surfaces. The exposed surfaces were mechanically polished up to 1200 grit SiC paper, then polished with a silica slurry and finally rinsed with ethanol. The composition of SBF was shown in Table 2. In this research, HCO_3^-, Cl^-, $H_2PO_4^-$ and SO_4^{2-} were focused. In order to investigate the influence of single ion on the corrosion behavior of WE43 alloy, test solutions with ion concentration magnification (ICM) 0.5, 1.0, 1.5, 2.0 and 2.5 times in SBF were prepared and shown in Table 3. Test specimens were subjected to nondeaerated aqueous solutions of $NaHCO_3$, $NaCl$, NaH_2PO_4 and Na_2SO_4 at room temperature. In the nondeaerated condition, the speciments were tested in the solutions open to air.

Electrochemical measurements were performed on electrochemical working station (PARSTAT®2273) with the conventional three electrode cell (a platinum foil as counter electrode and a saturated-calomel electrode as reference electrode). The open circuit potential (E_{ocp}) values of the specimens were monitored in the solutions for 36 ks. Potentiodynamic polarization tests were performed at a scan rate of 0.17mV/s. Electrochemical impedance spectroscopy (EIS) was carried out at range of 10mHz∼100kHz with 5 mV perturbation signal at the corrosion potential. To test the reliability and reproducibility of the measurements, duplicate experiments were performed in each case of the same conditions. For all the measurements, the same test was repeated at least twice.

Each corroded surface was observed using a Phillips XL30 scanning electron microscopy (SEM). The corrosion products on the surface were removed using a reagent of chromic acid cleaning solution containing of 220g/L Cr_2O_3+$AgNO_3$ at room temperature for 5-10min in order to remove the corrosion products without removing any amount of metallic Mg alloys.

Table 1. Chemical composition of WE43 alloy

Element	Y	RE[a]	Zr	Mg	Ni	Fe	Cu
Mass fraction (wt.%)	3.7-4.3	2.4-4.4	>0.4	Balance	<5ppm	<0 ppm	<20 ppm

[a] RE consists of Nd and heavy RE(Yb, Er, Dy, Gd)

Table 2. Composition of SBF

Component	NaCl	CaCl$_2$	KCl	MgSO$_4$	NaHCO$_3$	Na$_2$HPO$_4$	NaH$_2$PO$_4$
Conentration(g/L)	6.800	0.200	0.400	0.100	2.200	0.126	0.026

Table 3. Test solution with different ions

ICM / Ions species	0.5	1	1.5	2	2.5
Cl$^-$ / mol·L^{-1}	0.063	0.125	0.188	0.250	0.313
SO$_4^{2-}$ / mmol·L^{-1}	0.400	0.800	1.200	1.600	2.000
HCO$_3^-$ / mol·L^{-1}	0.013	0.026	0.039	0.052	0.065
H$_2$PO$_4^-$ / mmol·L^{-1}	0.110	0.220	0.330	0.440	0.550

3. RESULTS

100 μ
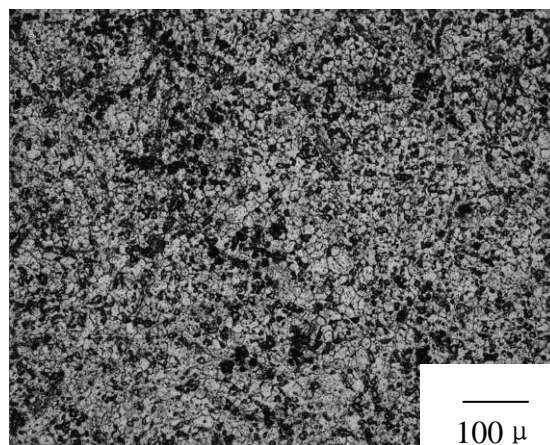
Figure 1. SEM images of the as-extruded WE43 alloy

Table 4. Mechanical properties of the as-extruded WE43 alloy

Alloy	UTS/MPa	YS/MPa	Elongation/%
WE43	280.5	205.6	9.2

Fig.1 shows the optical image of as-extruded WE43 alloy. In the hot extrusion process, it is a full dynamic recrystallization process, where more and diffusion second phase generated and made grains smaller. This WE43 alloy has better extension and yield strength (Table 4).

The open circuit potential (E_{ocp}) for WE43 alloy in different concentration of NaHCO$_3$, NaCl, NaH$_2$PO$_4$ and Na$_2$SO$_4$ solutions for 36 ks are shown in Fig.2. When WE43 alloy immerse in solutions, the protective film constitutes with Mg^{2+} and OH$^-$ ions is formed first, and then ions in SBF may react with substrate or surface film and participate in the corrosion process. The specimens exhibit a definite decrease in E_{ocp} values with the increase concentration of [Cl$^-$], [HCO$_3^-$], [H$_2$PO$_4^-$] and [SO$_4^{2-}$]. It implies that substrate or surface film may be attacked by these aggressive ions with time gradually.

Fig.3 shows potentiodynamic polarization curves of WE43 alloys immersed in NaHCO$_3$, NaCl, NaH$_2$PO$_4$ and Na$_2$SO$_4$ solutions. Generally the anodic reaction is the dissolution of Mg, occurred mainly on the broken area of the film.
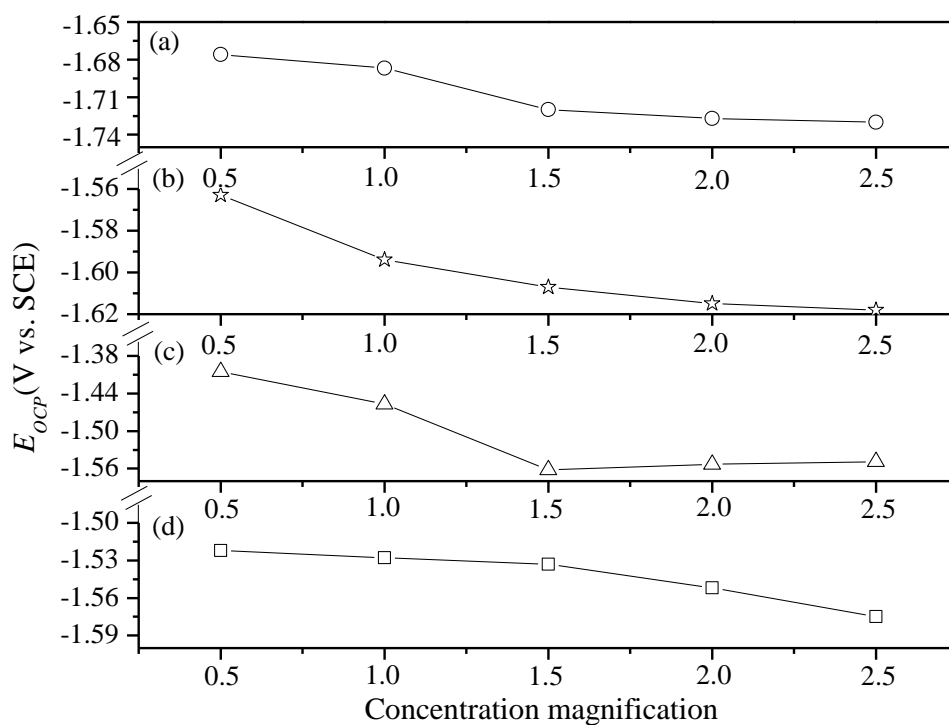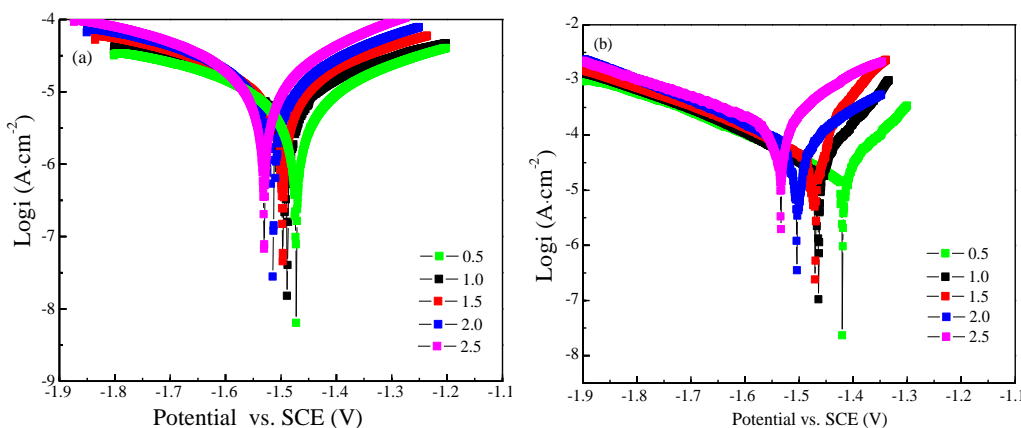

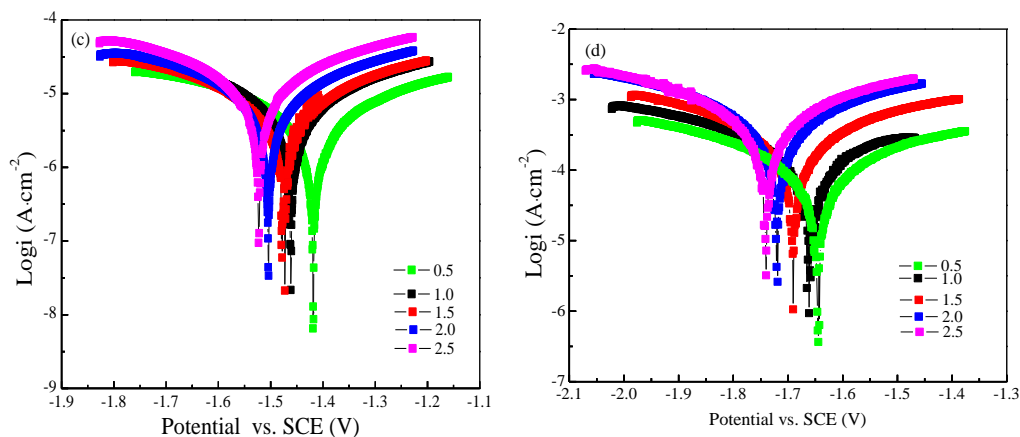**Figure 2.** Open-circuit potentials of WE43 alloy in various solutions (a) NaHCO$_3$, (b) NaCl, (c) NaH$_2$PO$_4$, (d) Na$_2$SO$_4$

Figure 3. Potentiodynamic polarization curves of WE43 alloy immersed in various solutions for 4h (a) NaHCO$_3$, (b) NaCl, (c) NaH$_2$PO$_4$, (d) Na$_2$SO$_4$
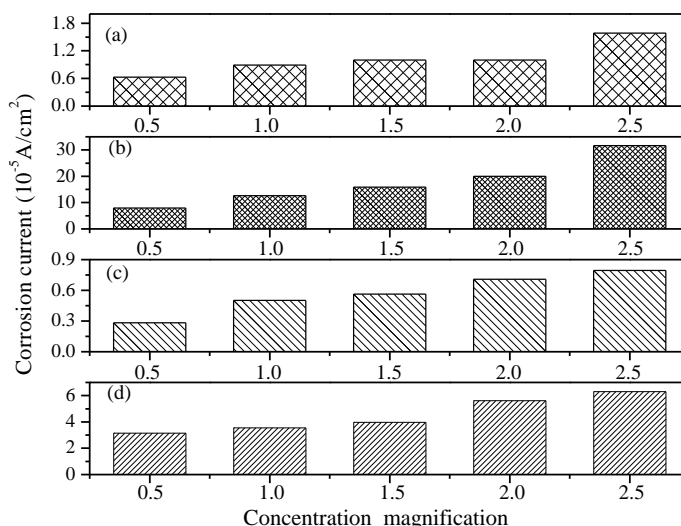

Figure 4. Corrosion current density of WE43 alloy immersed in various solutions (a) NaHCO$_3$, (b) NaCl, (c) NaH$_2$PO$_4$, (d) Na$_2$SO$_4$

Cathodic process may only make the surface film thinner with the hydrogen evolution occurred on the surface film [11, 12]. In NaCl solution, the anodic process is much more sensitive to Cl$^-$ ion than the cathodic process (Fig.3b). In NaHCO$_3$, NaH$_2$PO$_4$ and Na$_2$SO$_4$ solutions, specimens show similar cathodic and anodic polarization behavior. As the increase concentration of [HCO$_3^-$] [Cl$^-$], [H$_2$PO$_4^-$] and [SO$_4^{2-}$], the corrosion potential (E_{corr}) values shift to the negative direction, which accounts for the greater activity of the alloy [13]. This variation tendency is agree with that of E_{ocp} shown in Fig.2.

The calculated corrosion current density (I_{corr}) by Tafel extrapolation is shown in Fig.4. As concentrations of [HCO$_3^-$], [Cl$^-$], [H$_2$PO$_4^-$] and [SO$_4^{2-}$] increase, I_{corr} of specimens increase gradually. Corrosion rate has the relationship with corrosion current density as follows:

$$v = i \, / \, zFA = I_{corr}/zF \qquad\qquad (1)$$

Where v is corrosion rate; z is number of reaction electrons; F is faraday constant; A is electrode area. In the same reaction system, z and F are constants [14]. Therefore, the corrosion rate of WE43 alloy are enhanced by the increase concentration of aggressive ions and the order of ions etch resistance is $Cl^- > SO_4^{2-} > CO_3^- > H_2PO_4^-$.

To investigate the electrochemical corrosion mechanism in more detail, EIS are conducted with WE43 alloy electrodes immersed in various solutions for 4h, and the responses over a wide frequency range are recorded (shown in Fig.5). In $NaHCO_3$, NaH_2PO_4 and Na_2SO_4 solutions, the shape of data are characterized by two "depressed" capacitive loops at high and medium frequencies [15]. The high frequency loop is associated with the film of corrosion product, and the medium frequency loop could be due to charge transfer resistance and double layer capacitance, which form between the corroded layer and substrate. With the increase of ions concentration, the general shapes of these plots do not significantly change, indicating that the corrosion processes are not change obviously. Appropriate equivalent circuit Fig.6a is used to fit the EIS data shown in Fig.5a, 5c and 5d. The data are fit with ZSimpWin 3.10 software and the errors are less than 10%. This circuit consists of a resistor representing the electrolyte resistance R_s and two RC units in series that describe the interfacial properties of working electrode: R_{ct} refers to the charge transfer resistance and C_{dl} represents the electric double layer capacity at the interface of WE43 alloy subtrate and solution; R_f represents the film resistance and a constant phase element (CPE_f) is used to describe the film capacity.
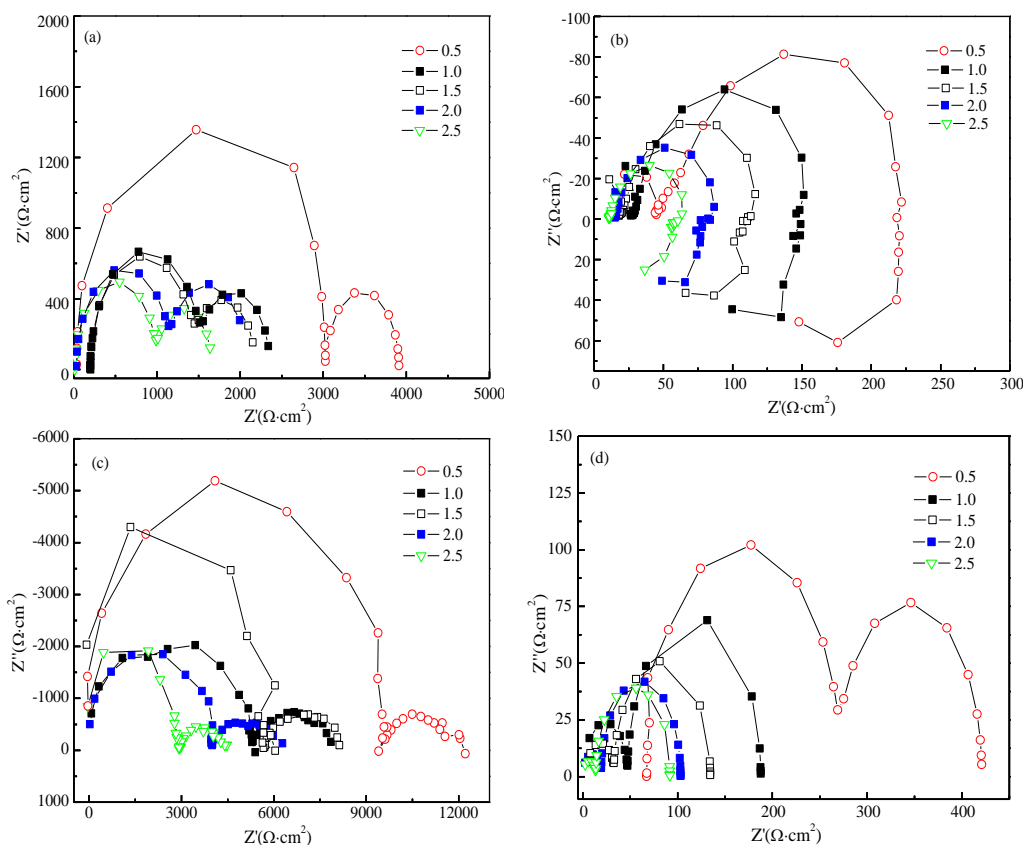

Figure 5. EIS of WE43 Mg alloys immersed in various solutions for 4h (a) $NaHCO_3$,(b) NaCl,(c) NaH_2PO_4,(d) Na_2SO_4

Fig.5b shows the EIS of WE43 alloy immersed in different concentration of NaCl ion solutions. The plot consists of one high frequency capacitance loop, one medium frequency capacitance loop and one low frequency inductive loop, which correspond to the characteristics of electric double layer, surface oxide film and the occurrence of pitting corrosion respectively [16].
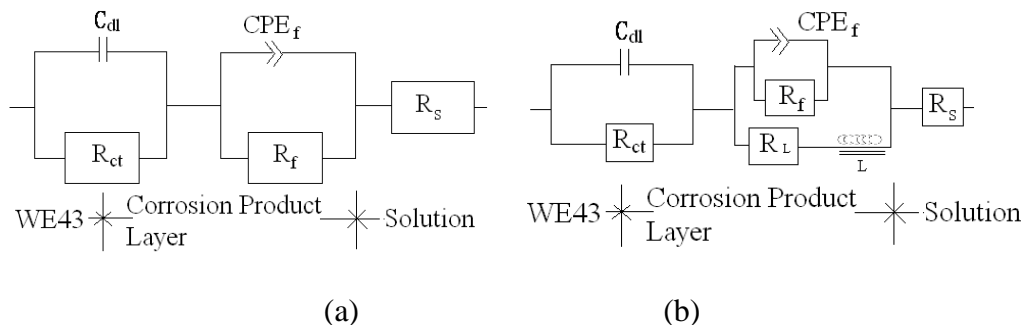

(a)   (b)

Figure 6. Equivalent circuits of WE43 alloy

Table 5. Fitting resulting of the EIS spectra

Ions species	ICM	$R_s(\Omega \cdot cm^2)$	$C_{dl}(\mu F \cdot cm^{-2})$	$R_{ct}(\Omega \cdot cm^2)$	$CPE_f(\mu F \cdot cm^{-2})$	$R_f(\Omega \cdot cm^2)$	$R_L(\Omega \cdot cm^2)$	$L(H \cdot cm^{-2})$
HCO_3^-	0.5	10^{-7}	6.89	3185	17.51	2121		
	1.0	10^{-7}	15.91	1869	19.04	1636		
	1.5	10^{-7}	15.72	1614	21.67	1588		
	2.0	10^{-7}	17.67	1326	22.75	1573		
	2.5	10^{-7}	25.73	1066	24.81	889.2		
Cl^-	0.5	3.47	12.81	141.6	99.85	73.9	130.6	90.04
	1.0	5.56	17.19	111.3	85.76	68.9	117.7	94.5
	1.5	6.67	18.07	81.8	85.26	48.7	89.9	102.9
	2.0	10.01	54.84	49.5	77.72	36.3	73.1	113.2
	2.5	10.23	71.92	37.8	60.07	24.45	60.3	137.3
$H_2PO_4^-$	0.5	7.05	21.5	3685	14.76	5135		
	1.0	8.84	29.8	3599	27.65	4402		
	1.5	9.95	32.3	2433	28.33	3072		
	2.0	8.86	33.5	1861	39.12	3068		
	2.5	9.88	85.4	1170	55.35	2909		
SO_4^{2-}	0.5	10^{-7}	17.05	226.0	3.53	199.8		
	1.0	10^{-7}	24.23	166.9	9.34	142.2		
	1.5	10^{-7}	25.47	48.29	20.21	132.2		
	2.0	10^{-7}	29.65	31.63	24.31	66.42		
	2.5	5.319	41.59	28.59	27.77	53.62		

The plot can be explained by the equivalent circuit shown in Fig.6b. R_L and L indicate the existence of metastable Mg^+ during the dissolution of Mg alloy substrate. In static corrosion test, corrosion product film $Mg(OH)_2$ formed at the outer surface firstly and protect substrate to some extent. The growth of $Mg(OH)_2$ layer is controlled by a dissolution-precipitation mechanism [17].

When Cl$^-$ ion exists in solutions, one hydration sheath composed of a row of water molecules formed on the surface of Mg alloy. Since Cl$^-$ ion is small enough, it displaces water molecule in the hydrogen sheath [18] and destroys the homeostasis of the dissolution-precipitation process. Therefore, Cl$^-$ ions preferentially combine with Mg^{2+} to transform Mg(OH)$_2$ into soluble MgCl$_2$. Fresh Mg alloy substrate is continuously generated and exposes to the solution resulted in continuous corrosion. The EIS implies that there is film layer formed on the WE43 surface incompletely and the dissolution of Mg substrate still carries out [19]. The fitting results are listed in Table 5. As the concentration of [HCO$_3^-$], [Cl$^-$], [H$_2$PO$_4^-$], [SO$_4^{2-}$] ions increase, the values of R_f and R_{ct} decrease; while the electric double layer capacity C_{dl} and film layer capacity CPE_f keep stable. In the immersion 4 hours, WE43 alloy occurs obviously pitting only in NaCl solution. As the concentration of Cl$^-$ ion arises from 0.063mol/L to 0.313mol/L, the decrease of R$_L$ and increase of L implies that the pitting on surface become seriously.
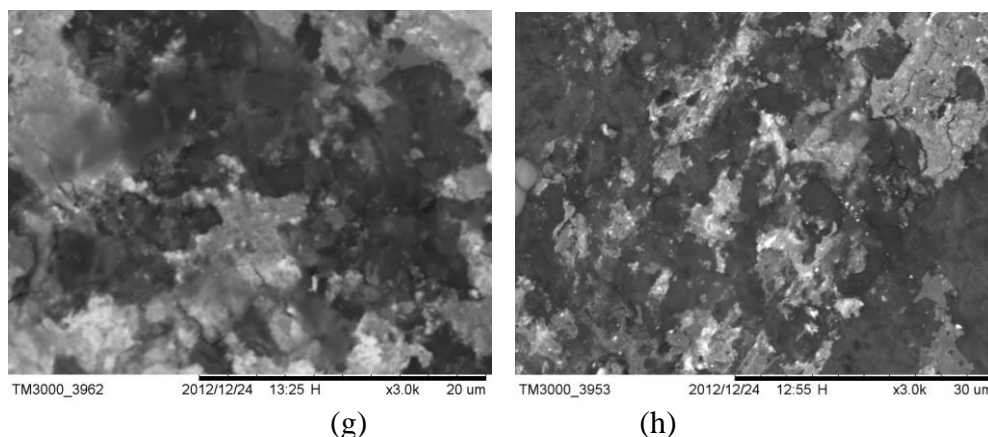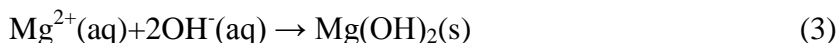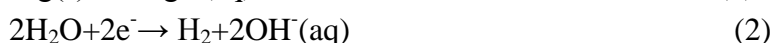

(a)

(b)

(c)

(d)

(e)

(f)

(g)   (h)
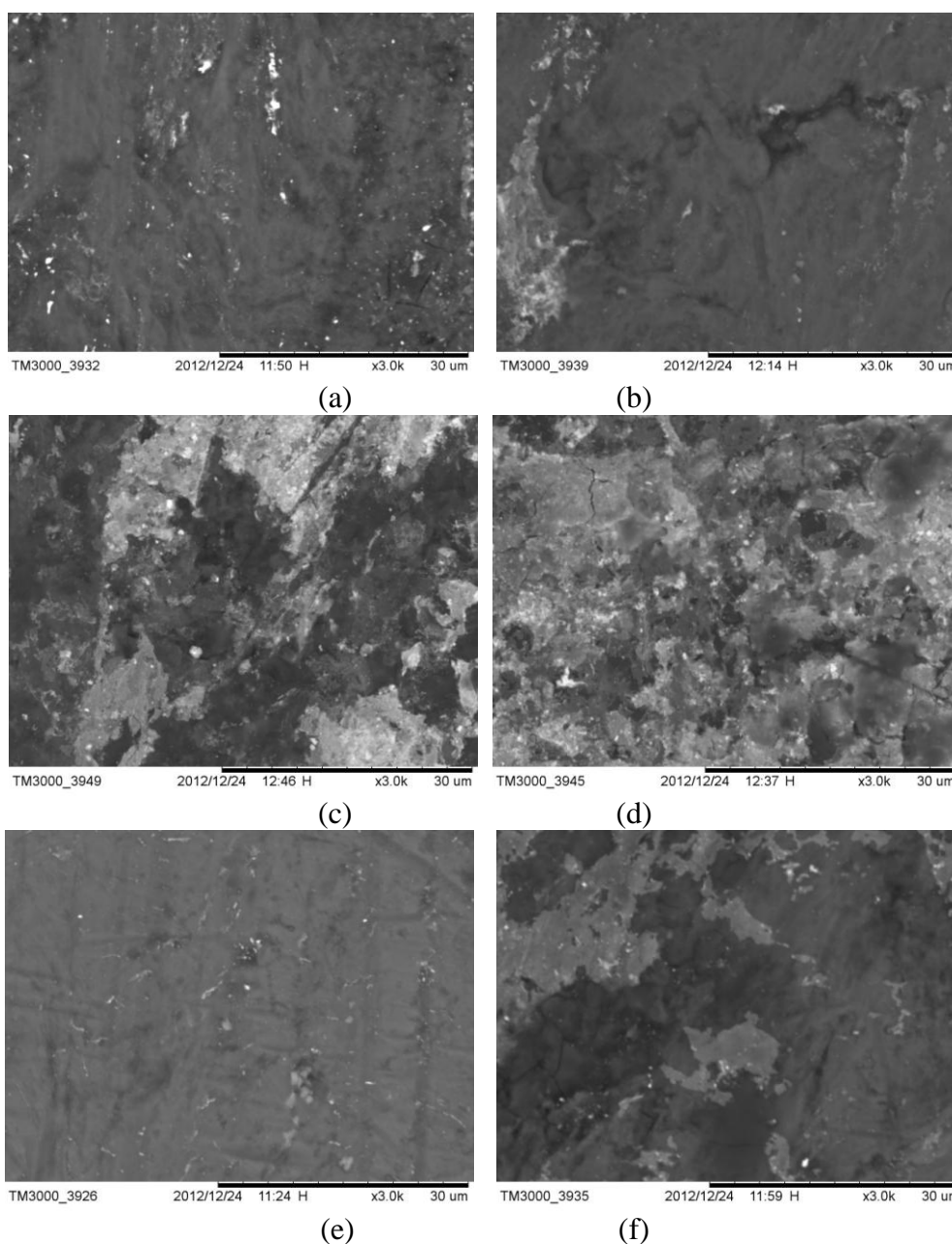
Figure 7. Corrosion morphology of WE43 alloy immersed in different solutions for 4h (a)HCO_3^- 0.013mol/L (ICM 0.5); (b)HCO_3^- 0.065mol/L (ICM 2.5); (c)Cl^- 0.063 mol/L(ICM 0.5); (d)Cl^- 0.313mol/L(ICM 2.5); (e)$H_2PO_4^-$ 0.11mmol/L (ICM 0.5); (f)$H_2PO_4^-$ 0.55mmol/L(ICM 2.5); (g)SO_4^{2-} 0.4mmol/L (ICM 0.5); (h)SO_4^{2-} 2.0mmol/L(ICM 2.5)

Corrosion morphology of WE43 alloy immersed in different solution for 4h is shown in Fig.7. The attack by HCO_3^- and $H_2PO_4^-$ ions are characterized by the formation of a crystalline-like film or product showing the general corrosion. The protolysis of HCO_3^- and $H_2PO_4^-$ ions counteract the development of pH gradients on the surface, resulted in the inhibition of pitting corrosion. Corrosion phenomenon is much pronounced in the solution containing Cl^- and SO_4^{2-} ions, which tend to enhance the dissolution of surface film. With the increase of ions concentration in solutions, non-uniform corrosion product layers are clearly visible over the entire surface of WE43 alloy.

4. DISCUSSION

Based on the results of electrochemical measurement and SEM, the effects of aggressive ions on the biodegradable mechanisms of WE43 alloy are discussed.

The Mg corrosion in a neutral solution undergoes the following reactions [15]:

$$Mg(s) \rightarrow Mg^{2+}(aq)+2e^- \qquad\qquad (1)$$
$$2H_2O+2e^- \rightarrow H_2+2OH^-(aq) \qquad\qquad (2)$$
$$Mg^{2+}(aq)+2OH^-(aq) \rightarrow Mg(OH)_2(s) \qquad\qquad (3)$$

In NaCl and Na_2SO_4 solutions, both Cl^- and SO_4^{2-} ions have good nucleophilicity and are easily adsorbed on the film [20]. As for the specimen in NaCl solution, localized corrosion may be viewed as the outcome of a competitive process between the inhibiting properties of hydroxyl ions and the breakdown-inducing effect of Cl^- ions [21, 22]. Cl^- ion is prone to drilling through the film and inducing pitting corrosion at microstructural defect sits because of their smaller radius [23].

$$w\ Mg^{2+}(aq) +z\ H_2O +2x\ OH^- +2y\ Cl^- \rightarrow 2Mg_w(OH)_xCl_y \cdot zH_2O \qquad (4)$$
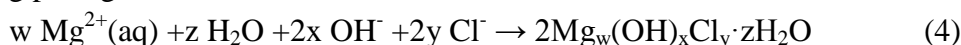
SO_4^{2-} ions may react with Mg^{2+} and produce soluble $MgSO_4$. Since the concentration of SO_4^{2-} ion is much lower 0.4-2.0mmol/L, the corrosivity is limited. As the concentration of Cl^- and SO_4^{2-} ions

increase, more corrosion products generate and dissolve in solutions, promoting the corrosion of WE43 alloy (Fig.7c,d,g,h).

In NaHCO$_3$ solution, magnesium carbonate product may be formed in NaHCO$_3$ solution (Eq.5). MgCO$_3$ is more stable with increasing of [HCO$_3^-$] ion as compared to Mg(OH)$_2$. The CO$_3^{2-}$ ion can enhance the destabilizaiton of Mg(OH)$_2$/MgO layer when [CO$_3^{2-}$] is relatively low as 4.76×10^{-4}mol/L. It suggests that CO$_3^{2-}$ ion is effective in retarding Mg dissolution by forming an insoluble MgCO$_3$ layer on the material when ion concentration is high enough [21], such as 0.013-0.065mol/L. From the Fig.7a and 7b, layers of corrosion products covered on alloys surface and made general corrosion.

$$Mg^{2+}(aq)+HCO_3^-(aq)+OH^-(aq) \rightarrow MgCO_3 + H_2O \qquad (5)$$
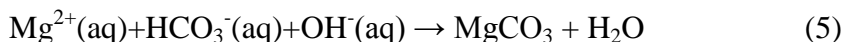
Moreover, Mg(OH)$_2$ is unstable in solution with pH less than 8.5 [24], then the magnesium hydroxyl carbonate such as Mg$_5$(CO$_3$)$_4$(OH)$_2 \cdot$8H$_2$O would be generated (Eq.6) [25].

$$5Mg(OH)_2(s)+4HCO_3^-(aq)+4H^+ \rightarrow Mg_5(CO_3)_4(OH)_2 \cdot 8H_2O \ (s) \qquad (6)$$

In NaH$_2$PO$_4$ solutions, the existence of H$_2$PO$_4^-$ ions can promote the dissolution of Mg. After the Eq.(1)-(2) occur in solution first, then reaction of Eq.(7) and (8) carry out and promote the reaction in Eq.(1).

$$H_2PO_4^- (aq) + 2OH^- (aq) \rightarrow PO_4^{3-} (aq) + H_2O \qquad (7)$$
$$HPO_4^{2-} (aq) + OH^- (aq) \rightarrow PO_4^{3-} (aq) + H_2O \qquad (8)$$

The reaction of Eq.(7) and (8) can promote the Mg dissolution(Eq.(1)). However, the solubility product constant K$_{sp}$ for Mg$_3$(PO$_4$)$_2$ is 1.04×10^{-24}, which is much lower than the K$_{sp}$ of other products. Thus, PO$_4^{3-}$ will preferentially bond with Mg^{2+} to form the white compound of Mg$_3$(PO$_4$)$_2$, and then white compounds adhere onto the surface of Mg(OH)$_2$ film (Fig.7f). Song et al. has reported the presence of Mg$_3$(PO$_4$)$_2$ and Ca$_{10}$(PO$_4$)$_6$(OH)$_2$ in the corrosion layer on Mg alloy immersed in SBF [17].

5. CONCLUSIONS

Many ions in SBF can attack WE43 alloy and participate in the constituent of corrosion product. In this paper, effects of aggressive ions such as [HCO$_3^-$], [Cl$^-$], [H$_2$PO$_4^-$] and [SO$_4^{2-}$] ions on the corrosion behavior of WE43 alloy were investigated.

(1) In the initial stage, as the concentration of [HCO$_3^-$], [Cl$^-$], [H$_2$PO$_4^-$] and [SO$_4^{2-}$] ions increased, E_{ocp} and E_{corr} of WE43 alloys specimen shifted to the negative direction, and the I_{corr} increased, accounts for the greater activity of the alloy.

(2) The order of ions corrosivity for WE43 alloy immersed in SBF is [Cl$^-$] >[SO$_4^{2-}$] >[HCO$_3^-$] >[H$_2$PO$_4^-$]. Corrosion phenomenon is much pronounced in the solution containing Cl$^-$ and SO$_4^{2-}$ ions, which tended to enhance the dissolution of surface film. The formation of crystalline like MgCO$_3$ products exhibited the general corrosion in NaHCO$_3$. Moreover, WE43 alloy has a better corrosion resistance in NaH$_2$PO$_4$, attributed to the lower concentration of [H$_2$PO$_4^-$] in SBF.

References

1. X.B. Zhang, G.Y. Yuan, L. Mao, J.L. Niu, W.J. Ding, *Mater. Lett.*, 66(2012)209.
2. G. Mani, M. D. Feldman, D. Patel, C. M. Agrawal, *Biomater.*,28(2007)1689.
3. M.P. Staiger, A.M. Pietak, J. Huadmai, G. Dias, *Biomater.*, 27(2006)1728.
4. F. Witte, V. Kaese, H. Haferkamp, E. Switzer, A. Meyer-Lindenberg, C. Wirth, H. Windhagen. *Biomater.*, 26(2005)3557.
5. T. Rzychon, J. Michalska, A. Kielbus, *J. Achv. Mater. Manuf. Eng.*, 21 (2007)51.
6. C. D. Mario, P. Barlis, J. Tanigawa, *Eur. Heart J.*, 28 (2007)2319.
7. L.J. Liu, M. Schlesinger, *Corros. Sci.*, 51(2009)1733.
8. M. JÖsson, D. Persson, *Corros. Sci.*, 52(2010)1077.
9. P.J. Uggowitzer, A.V. Nagasekhar, P. Schmutz, M. Easton, G. L. Song, A. Atrens, M. Liu, *Corros. Sci.*, 51(2009)602.
10. C.H. Ye, Y.F. Zhenga, S.Q. Wangc, T.F. Xi, Y.D. Li, *Appl. Surf. Sci.*, 258 (2012)3420.
11. G. Song, A. Atrens, M. Dargusch, *Corros. Sci.*, 41(1998)249.
12. Y.W. Song, D.Y. Shan, R.S. Chen, E.H. Han, *Corros. Sci.*,51(2009)1087.
13. E. Brillas, P.L. Cabot, F. Centellas, J.A.Garrido, E. Pérez, R.M. Rodríguez, *Electrochim. Acta*, 43(1998)799.
14. H. Yang, W.Q. Lu. Applied Electrochemisty, China: Science press, 2010, 157.
15. L. Wanga, T. Shinoharab, B. Zhang, *J. Alloy. Compd.*, 496 (2010)500.
16. G. Ballerini, U. Bardi, R. Bignucolo, G. Ceraolo, *Corros. Sci.* 47 (2005)2173.
17. Y.W. Song, D. Shan, R. Chen, F. Zhang, E.H. Han, *Mater. Sci. Eng. C*, 29 (2009)1039.
18. A. Pardo, M. C. Merino, A.E. Coy, R.Arrabal, F.Viejo, E. Matykina, *Corros. Sci.*,50(2008)823.
19. X. Zhang, G. Yun, L. Mao, J. Niu, W. Ding, *Mater. Lett.*, 66(2012)209.
20. S. Ono, H. Habazaki, *Corros. Sci.*, 51(2009)2364.
21. S.M. Abd El Haleem, S. Abd El Wanees, E.E. Abd El Aal, A. Diab, *Corros. Sci.*, 52(2010)292.
22. H.P. Godard, W.B. Lepson, M.R. Bothewell, the Corrosion of Light Metals, Wiley, New York, 1967, 260.
23. S. Singh, S. Basu, A. K. Poswal, R.B.Tokas, S.K.Ghosh, *Corros. Sci.*, 51(2009)575.
24. X.Z.Yang, W.Yang, Electrochemical Thermodynamics of Metal Corrosion, Chemical Industry Publishing House, Beijing,1991,10.
25. M. Jönsson, D. Persson, D. Thierry, *Corros. Sci.* 49 (2007)1540.